PCCP

Accepted Manuscript

ROYAL SOCIETY OF CHEMISTRY

www.rsc.org/pccp

Cite this: DOI: 10.1039/c0xx00000x

www.rsc.org/xxxxxx

ARTICLE TYPE

Dynamic Study of binary Network Structural Change in Response to Guest Inclusion

Min Li[a,b,‡], Peng Xie[a,‡], Ke Deng[b], Yan-Lian Yang[b], Sheng-Bin Lei[c], Zhong-Qing Wei[a,*], Qing-Dao Zeng[b,*] and Chen Wang[b,*]

Received (in XXX, XXX) Xth XXXXXXXXX 20XX, Accepted Xth XXXXXXXXX 20XX

DOI: 10.1039/b000000x

In the present work flexible binary networks of 1,3,5-benzenetricarboxylic acid (TMA) with 4,4'-bipyridine (Bpy) or 1,3,5-tris(4-pyridyl)-2,4,6-triazine(TPTZ) molecules at the liquid-solid interface were constructed. When coronene (COR) molecules are introduced into these systems, the binary networks collapse and at the same time, new COR/TMA host-guest structures are formed. Both experiments and calculations unambiguously indicate that the COR/TMA host-guest complex structure has stronger adsorption energy, resulting in the deconstruction/reconstruction phenomenon.

Introduction

Self-assembled 2D networks have received a lot of attention in recent years due to their broad range of potential applications, which has greatly expanded knowledge in the field of physisorbed, self-assembled molecular systems.[1-4] The well-ordered networks at surfaces and interfaces can act to immobilize and isolate functional objects at the molecular scale [2, 5-7]. They can also serve as an ideal matrix to study the dynamics of guest binding, diffusion, and manipulation by scanning probe microscopy [8-10]. Recent studies have also demonstrated that the multi-component molecular assemblies could inspire new molecular architectures for guest molecule inclusion,[2, 11-13] or novel designs of metal-organic-frameworks (MOFs).[14] In addition, the flexible bone networks are of great significance in bioactive compound recognition, which has attracted much attention recently.[15, 16] Nevertheless, the vast majority of reported network host-guest systems are focused on rigid molecular networks with permanent porosities. In contrast, less work has been done on flexible networks which can involve conformational change on adsorption or even the pronounced structural transformation arising from competitive adsorption at solid-liquid interfaces in response to guest inclusion.[17] In the present work, we construct flexible binary networks on a highly oriented pyrolytic graphite (HOPG) surface and demonstrate, by introducing a guest molecule, that the competitive adsorption among components determines the observed collapse of molecular patterning and subsequent layer reconstruction. Scanning tunneling microscopy (STM) is employed to investigate the dynamics involved in the surface self-assembly process at a molecule level. [18, 19]

In this work, 4,4'-bipyridine (Bpy) and 1,3,5-tris(4-pyridyl)-2,4,6-triazine (TPTZ) were chosen to mediate the network characteristics of 1,3,5-benzenetricarboxylic acid (TMA), as pyridine derivatives are well known to form various complex structures with the molecules containing carboxylates.[20-23] The basic assembly blocks consist of acid-bipyridine-acid units that can be resolved with sub-molecular resolution with the aid of STM. A guest molecule, coronene (COR), was introduced into this system to investigate the properties of these binary networks. Additionally, a rational explanation is presented based on density functional theory (DFT) calculations.

Experimental

The materials used in the experiments, TMA, Bpy, TPTZ and coronene (COR) (molecular structures shown in Figure 1) were purchased from Acros Co. and used without further purification. The solvents used in this work were 1-heptanoic acid (AR) and phenyloctane (>98%, purchased from Acros Co.).

The mixture of TMA and Bpy (or TPTZ) was dissolved in 1-heptanoic acid at a concentration of 10^{-4} M. The samples were prepared by depositing a droplet of the above solution on a basal plane of a freshly cleaved highly oriented pyrolytic graphite (HOPG) surface. Then, a droplet of the solution of COR in phenyloctane with a certain concentration was added on top of an already existing TMA/Bpy network pattern on the surface for the host-guest complexation. STM experiments were carried out with a Nanoscope IIIa scanning probe microscope system under ambient conditions (Bruker, USA). Tips were mechanically cut from Pt/Ir wires (80/20). All STM images were recorded in the constant current mode.

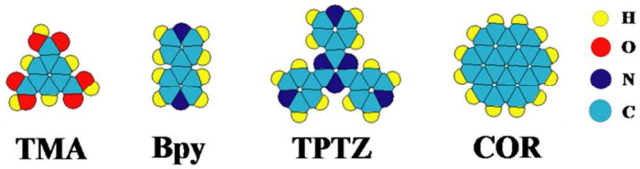

Fig.1 Chemical structures of the adsorbate molecules: 1,3,5-benzenetricarboxylic acid (trimesic acid, TMA, $C_9H_6O_6$), 4, 4'-bypyridine (Bpy, $C_{10}H_{10}N_2$), 1,3,5-tris(4-pyridyl)-2,4,6-triazine (TPTZ, $C_{18}H_{12}N_6$) and coronene (COR, $C_{24}H_{12}$).

Theoretical calculation methods

We performed periodic theoretical calculations using density functional theory (DFT) provided by the DMol3 code. [24] We use the periodic boundary conditions (PBC) to describe the 2D periodic structure on the graphite in this work. The Becke exchange gradient correction and the Perdew–Wang correlation

gradient correction are applied in the generalized gradient approximation (GGA) to describe exchange and correlation. [25] We expand the all-electron spin-unrestricted Kohn-Sham wave functions in a local atomic orbital basis. In such double-numerical basis set, polarization is described. All calculations are all-electron ones and performed with the Extra-Fine mesh. Self-consistent field procedure is done with a convergence criterion of 10^{-5} a.u. on the energy and electron density.

Results

Assembly of TMA / Bpy and TMA / TPTZ networks on HOPG surface

1,3,5-benzenetricarboxylic acid formed an open honeycomb supramolecular network in 1-heptanoic acid on HOPG surface as illustrated in Figure 2a and as reported by W. M. Heckl et al.[26] When mixing TMA with 2-fold symmetric Bpy at a heptanoic acid / graphite interface, a well-ordered rectangular network structure is instead formed as revealed in Figure 2b, which is very different from the 2D hexagonal honeycomb formed from pure TMA (Figure 2c). Each TMA molecule links with two neighboring TMA molecules through two pairs of O•••H-O hydrogen bonds, forming a zigzag chain-like pattern as marked by the yellow line on the STM image in Figure 2c. Meanwhile the Bpy molecule acts as a bridge to connect two TMA molecules on both sides via intermolecular N•••H-O hydrogen bonds, resulting in the formation of binary rectangular networks. The observed structure can be attributed to units of TMA-Bpy-TMA trimers which are consistent with the previously reported acid-bipyridine-acid motifs. [20-23] It was found that adjusting the molar ratio of TMA to Bpy from 2:3 to 2:9 does not affect the outcome of TMA-Bpy complex self-assembly behavior, indicating that this network pattern is thermodynamically favored. In this work, a slight excess of Bpy in solution in this work (That is, the ratio of TMA to BPY varied from 2:3 to 2:4) was used to construct a perfect TMA/BPY binary network for the subsequent COR inclusion since a slightly less Bpy in solution could result in some narrow rows formed from pure TMA in the binary monolayer as shown in Figure S1. It should be noted that our previous studies showed that TMA and Bpy molecules prefer to form close-packed lamella on HOPG surfaces when using toluene as the solvent [20], which is very different from the structures assembled from 1-heptanoic acid here. Figure 2d is the molecular model suggested on the basis of the STM observations. The unit cell is also superimposed on the molecular model with a = 2.80 nm, b = 1.81 nm, α = 113.6°. The inner width of the cavity is m = 1.95 nm, n = 0.96 nm.

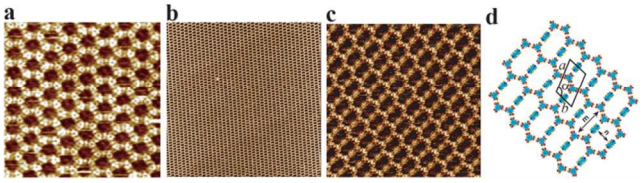

Fig. 2 (a) Constant current STM image (12.7 nm ×12.7 nm) of a self-assembled networks of TMA at 1-heptanoic acid / HOPG interface. The imaging conditions are I = 498 pA and V = 800 mV. (b) STM image (100 nm × 100 nm) of an ordered network of Bpy/TMA at 1-heptanoic acid / HOPG interface. The imaging conditions are I = 531 pA and V = 688 mV. (c) A higher resolution STM image (20 nm × 20 nm) of the binary assembly structure. The imaging conditions are I = 532 pA and V = 700 mV. (d) Suggested molecular model of BPY/TMA binary assembly.

TPTZ is a similar ligand molecule but with 3-fold symmetry compared with 2-fold symmetric Bpy. TPTZ typically forms uniform hexagonal network structures when adsorbing at a 1-heptanoic acid / HOPG interface, as shown in Figure 3a. Based on the high-resolution STM image (inset, Figure 3a), it is clearly seen that the cavity with good 6-fold symmetry is surrounded by six TPTZ molecules (triangular-featured spots) via non-covalent interaction which could be attributed to N•••H-C hydrogen bonding.

It is expected that when mixing TMA with 3-fold symmetric TPTZ molecule at a liquid/solid interface, a network structure with 3-fold symmetry would form. The corresponding binary structure from TPTZ and TMA when co-adsorbing at 1-heptanoic acid/HOPG interface is presented in Figure 3b, which is similar to the work reported by Markus et al. [27] A cartoon model of the TMA molecule (blue circle) and the TPTZ molecule (red triangle) is superimposed on the STM image. An inset in Figure 3b shows the details of this network structure. Three TPTZ molecules are alternatively linked with three TMA molecules through N•••H-O hydrogen bonds, forming a larger cavity than pure TMA itself. A model of the assembling structure indicating

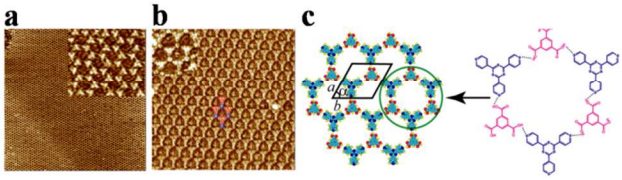

the H-bonding scheme is depicted in Figure 3c. The unit cell is also superimposed on the molecular model with a = b = 2.08 nm, α = 120°.

Fig. 3 (a) STM image (170 nm × 170 nm) of an ordered hexagonal network of TPTZ at 1-heptanoic acid / HOPG interface. The scanning conditions are I = 562 pA and V = 716 mV. (b) STM image (20 nm × 20 nm) of TPTZ/TMA network structure. The scanning conditions are I = 546 pA and V = 553 mV. (c) Suggested molecular model of TPTZ/TMA binary assembly. On the right of the model, the hydrogen bonds between TPTZ and TMA molecules are indicated by the black dot lines.

Collapse of TMA / Bpy and TMA / TPTZ networks and structural re-organisation upon guest inclusion

To further investigate the properties of the 2D binary networks, a planar molecule, coronene (COR), was introduced into the two assembling systems. The volume and concentration of the host binary components as well as the added COR droplet were carefully controlled for good reproducibility. For the TMA/Bpy mixture, a 2 μl droplet of the solution (10^{-4} M) was previously introduced onto HOPG surface to form a uniform rectangular network before applying 0.5 μl COR solution in phenyloctane

with a concentration of 10^{-5} M into the system. Figure 4a-j shows the dynamic process of the binary structure collapse and new structure formation upon inclusion of COR molecules. The droplet of COR was added in situ during imaging of the binary network. The white line marked by the two small arrows in Figure 4a indicates a momentary disturbance after introducing the guest solution to the system during scanning. Immediately after COR molecule inclusion (within 5s), one can clearly see the structural change especially at the boundary of different domains at the lower part under the white line in Figure 4a. The fast structural change, the reconstruction at the boundary, is

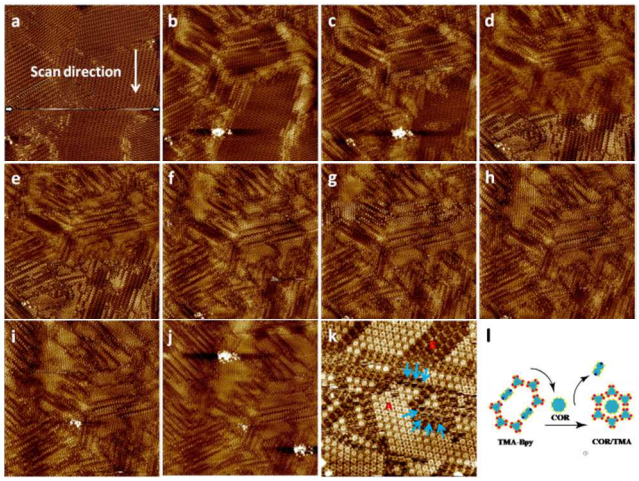

Fig. 4 (a)-(j) The time-dependent dynamic process of the COR/TMA host-guest structure formation when COR molecules were introduced into TMA-Bpy complex system. The scan area is 100 nm × 100 nm for each STM image. (k) A higher resolution STM image (33.4 nm × 33.4 nm) of COR/TMA (A domain) and TMA-Bpy (B domain) assembly structures. The imaging conditions are I = 540 pA and V = 1024 mV. (l) Schematic diagram for this competitive adsorption process.

pronounced in Figure 4b compared with the empty binary network in the upper part of Figure 4a. Based on Figure 4a-4c, the domain boundary is the preferential place for commencement of network collapse and new COR/TMA complex formation, indicating less stable adsorption of the former network molecules at the boundary. The STM images (Figure 4a-j) were scanned continuously, each taking 85s in total. A detailed re-assembled structure is clearly observed in the higher resolution STM image (Figure 4k) including domains A and B. In domain A, the COR molecule was not included in the rectangular binary network but in the re-constructed hexagonal TMA network, indicating the COR/TMA complex on graphite is the system with minimum Gibbs free-energy. Taking a closer look at the location of the entrapped COR molecules, one can clearly see the coronene molecule appears as round feature with a diameter of ~1 nm and is surrounded by six TMA molecules through six pairs of C-H•••O hydrogen bonds, thus forming the COR/TMA host-guest structure. There are also some empty cavities formed by six TMA molecules (indicated by the blue arrows), in which some COR molecules might have been removed by the tip during scanning. In domain B, in which the assembling structure is not disturbed by the COR molecules, the rectangular network still remains. Both the TMA and Bpy molecules are clearly distinguished in the STM image. The area of domain A keeps growing with time based on Figure 4a-4j.

For the TMA/TPTZ mixture, COR molecules were introduced in a same way to the case of TMA/Bpy. Figure 5a-o shows the whole dynamics process after COR molecules were added in this way to the system. All the STM images were continuously scanned. The scan time for each image is 75s. More TPTZ molecules were desorbed from the binary assembled network into the solution with time. Meanwhile, the COR/TMA complex

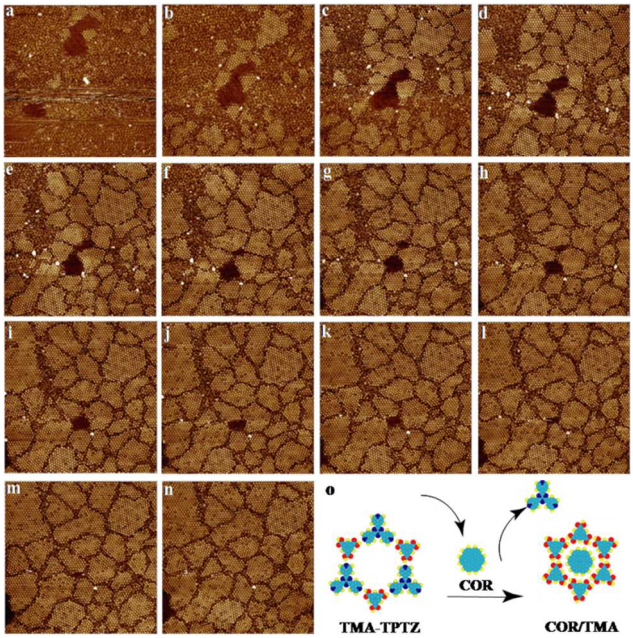

Fig. 5 (a)-(n) The time-dependent dynamic process of the COR/TMA host-guest structure reconstruction when COR molecules were added into TMA-TPTZ assembly system. The scan area is 100 nm × 100 nm for each STM image. (o) Schematic diagram for this dynamic layer reconstruction.

structure reassembled and covered more surface with time. It should be noted that the structural transformation of TMA/TPTZ binary network in response to COR molecules inclusion is similar to that of TMA/Bpy system but not the same. In TMA/Bpy system, one can clearly observe the structural transformation during scanning as shown in Figure 4. However, for TMA/TPTZ system, TMA/TPTZ binary network becomes disordered immediately after COR molecules is added, which makes it difficult to get higher resolution image of the host structure after adding guest molecules (Figure S2). The different phenomenen observed in both binary structural transformations could be due to different building motifs (Figures 2d and 3c) which might determine the process of the structure transformation.

Discussion

The adsorbates within the self-assembled monolayer on HOPG surface dynamically equilibrate with the molecules in the above solution. After introducing a guest molecule which has a strong interaction with the host assembling structure as well as the substrate, the equilibrium will be perturbed. Stable adsorption of molecular monolayers at the liquid-solid interface only takes place in an equilibrium situation when the system minimizes free

energy. To augment the STM observations, DFT calculations (see details in the Theoretical calculation methods part and SI) were carried out based on the models of physisorbed molecules on HOPG (Figure S3) to understand both the stability of the binary network and the effect of adding the guest molecule into this system in the presence of the substrate (Table 1). Though it cannot be ignored, the effect of solvents was not taken into account owing to the impossibility for DFT calculation.

According to the calculation results, the binding energy for the TMA network is 97.86 kJ mol^{-1} nm^{-2} which is much larger than that for TMA-Bpy (68.04 kJ mol^{-1} nm^{-2}). Here, we should note that it is not surprising the TMA-Bpy binary network can still form though it is much less stable than pure TMA network according to the calculation results, since the contribution of the solvent molecules (heptanoic acid) to the stability of the binary network is not considered as mentioned above. The complex of COR with the TMA network further facilitates the adsorption through an increased adsorption energy (15.54 kJ mol^{-1} nm^{-2} for COR/TMA compared to 0.24 kJ mol^{-1} nm^{-2} for COR/TMA-Bpy). Considering the interaction between adsorbates and the substrate, TMA network-graphite possesses stronger adsorption energy (30.70 kJ mol^{-1} nm^{-2}), than TMA-Bpy binary network-graphite (23.62 kJ mol^{-1} nm^{-2}). It should be noted that the lower interaction (23.62 kJ mol^{-1} nm^{-2}) between TMA-Bpy and COR could be due to the lesser width of the cavity into which it is difficult for COR to enter. Thus, the total interaction energy of TMA/COR with graphite is 144.1 kJ mol^{-1} nm^{-2} while for TMA/Bpy/COR-graphite it is 91.90 kJ mol^{-1} nm^{-2}. Apparently, the former has stronger competitive adsorption than the latter, which accounts for the STM observation that the binary TMA/Bpy network collapses in response to guest inclusion and finally re-assembles with the guest molecule into the new TMA/COR supramolecular architecture.

Table 1. Energy calculations for adsorbates on HOPG surface

	Template network [kJ mol^{-1} nm^{-2}]	Template network-COR [kJ mol^{-1} nm^{-2}]	Template network-graphite interaction [kJ mol^{-1} nm^{-2}]	Total Interaction [a] [kJ mol^{-1} nm^{-2}]
TMA	97.86	15.54	30.70	144.1
TMA-Bpy	68.04	0.24	23.62	91.90
TMA-TPTZ	47.04	3.78	20.46	71.28

[a] *For these three kinds of networks, TMA, TMA/Bpy and TMA/TPTZ, the interaction of COR with graphite was not involved since COR molecules could not entrap into both TMA/Bpy and TMA/TPTZ networks. Therefore, the binding energy of COR to graphite was not counted in the total interaction for the three systems.*

For the TPTZ-TMA system, the binding energy of the TPTZ-TMA network is 47.04 kJ mol^{-1} nm^{-2}, which is much weaker than that of TMA, indicating that the network formed by the two components is less stable. It is understandable that low-density structures are not optimal from the viewpoint of Gibbs free energy. This is further demonstrated by introducing the COR molecules according to both the STM observation and theoretical calculations (0.24 kJ mol^{-1} nm^{-2} for COR/TMA-TPTZ compared to 15.54 kJ mol^{-1} nm^{-2} for COR/TMA). The TMA-TPTZ network on graphite is less stable (20.46 kJ mol^{-1} nm^{-2}) than TMA-graphite (Table 1), possibly due to the lower number of absorbing molecules on the surface per unit area. In addition, the interaction between the TMA-TPTZ network and COR is very weak (3.78 kJ mol^{-1} nm^{-2}), which might be interpreted as a less stable adsorption of COR molecules in the large cavity. As a result, the total interaction of TMA/TPTZ/COR with graphite is 71.28 kJ mol^{-1} nm^{-2} which is much less than that of TMA/COR with graphite.

The theoretical calculation results give a rational explanation for the reconstruction phenomenon observed in our work. The stability of the multi-component supramolecular structure must be taken into account when constructing multi-component molecular assemblies. This difference is small for one single molecule, but significant for the total system. Such calculations can thus be a guide to predicting the formation of complex and functional heterogeneous molecular architectures.

Conclusions

In summary we have shown that in Bpy/TMA or TPTZ/TMA binary systems, TMA-Bpy(TPTZ) molecules exclusively form 2D binary networks via N•••H-O intermolecular hydrogen bonds between carboxyl and pyridine groups at the liquid-solid interface. When introducing coronene (COR) molecules into these systems, the flexible networks can collapse and at the same time, new COR/TMA host-guest structures are formed. Both experiments and calculations unambiguously indicate that the COR/TMA host-guest complex structure has stronger adsorption energy, resulting in the reconstruction phenomenon. These results give us an improved understanding of the interactions between guest molecules and the template, as well as the substrate, and will lead to a better comprehension of the concept of competitive adsorption for the fabrication of functional molecular arrays. Most importantly we demonstrate the dynamic response of 2D molecular networks on surfaces to environment stimuli which has critical technological and economic importance.

Acknowledgements

M.L. acknowledges the Fund from the National Basic Research Program of China (Nos. 2011CB933101, 2011CB932303). Financial supports from the Hundred Elites Program of the Chinese Academy of Sciences, National Natural Science Foundation of China (grant no. 21303208, 21073048, 51173031) and the Start-Up Funding from the Institute of High Energy Physics of the Chinese Academy of Sciences (No. 2011IHEPYJRC504) are also gratefully acknowledged.

Notes and references

[a] *CAS Key Laboratory for Biomedical Effects of Nanomaterials and Nanosafety, Institute of High Energy Physics, the Chinese Academy of Sciences, Beijing 100049, P. R. China. E-mail: zwei@ihep.ac.cn*

[b] *CAS Key Laboratory of Standardization and Measurement for Nanotechnology, National Center for Nanoscience and Technology, Beijing 100080, China. E-mail: zengqd@nanoctr.cn;wangch@nanoctr.cn*

[c] *Key Laboratory of Microsystems and Microstructures Manufacturing, Ministry of Education, Harbin Institute of Technology, Harbin, 150080, China.*

‡ *These authors contribute to this work eaqually.*

1 G. Pawin, K. L. Wong, K. Y. Kwon, and L. Bartels, *Science*, 2006, **313**, 961.

2 J. A. Theobald, N. S. Oxtoby, M. A. Phillips, N. R. Champness, and P. H. Beton, *Nature*, 2003, **424**, 1029.

3 D. Bonifazi, S. Mohnani, and A. L. Pallas, *Chem. Eur. J.*, 2009, **15**, 7004.

4 T. Kudernac, S. B. Lei, J. A. A. W. Elemans, and S. De Feyter, *Chem. Soc. Rev.*, 2009, **38**, 402; J. A. A. W. Elemans, S. B. Lei, and S. De Feyter, *Angew. Chem. Int. Ed*. 2009, **48**, 7298.

5 S. Stepanow, M. Lingenfelder, A. Dmitriev, H. Spillmann, E. Delvigne, N. Lin, X. B. Deng, C. Z. Cai, J. V. Barth, and K. Kern, *Nat. Mater.*, 2004, **3**, 229.

6 J. Adisoejoso, K. Tahara, S. Okuhata, S. B. Lei, Y. Tobe, and S. De Feyter, *Angew. Chem. Int. Ed.*, 2009, **48**, 7353.

7 M. Li, K. Deng, S. B. Lei, Y. L. Yang, T. S. Wang, Y. T. Shen, C. R. Wang, Q. D. Zeng, and C. Wang, *Angew. Chem. Int. Ed*., 2008, **47**, 6717.

8 W. Ho, *J. Chem. Phys.*, 2002, **117**, 11033.

9 M. Ruben, D. Payer, A. Landa, A. Comisso, C. Gattinoni, N, Lin, J. P. Collin, J. P. Sauvage, A. De Vita, and K. Kern, *J. Am. Chem. Soc.*, 2006, **128**, 15644.

10 S. J. H. Griessl, M Lackinger, F. Jamitzky, T. Markert, M. Hietschold, and W. M. Heckl, *J Phys Chem B*, 2004, **108**, 11556.

11 L. Kampschulte, S. Griessl, W. M. Heckl, and M. Lackinger, *J. Phys. Chem. B*, 2005, **109**, 14074.

12 K. G. Nath, O. Ivasenko, J. A. Miwa, H. Dang, J. D. Wuest, A. Nanci, D. F. Perepichka, and F. Rosei, *J. Am. Chem. Soc.*, 2006, **128**, 4212.

13 Y. L. Yang, and C. Wang, *Int. J. Nanotechnology*, 2007, **4**, 4; Y. B. Li, K. Q. Zhao, Y. L. Yang, K. Deng, Q. D. Zeng, and C Wang, *Nanoscale*, 2012, **4**, 148

14 H. Furukawa, K. E. Cordova, M. O'Keeffe, and O. M. Yaghi, *Science*, 2013, **341**, 974; H. X. Deng, S. Grunder, K. E. Cordova, C. Valente, H. Furukawa, M. Hmadeh, F. Gándara1, A. C. Whalley, Z. Liu, S. Asahina, H. Kazumori, M. O'Keeffe1, O. Terasaki, J. F. Stoddart, and O. M. Yaghi, *Science*, 2012, **336**, 1018; H. Furukawa1, N. Ko, Y. B. Go, N. Aratani, S. B. Choi, E. Choi, A. Özgür Yazaydin, R. Q. Snurr, M. O'Keeffe1, J. Kim, and O. M. Yaghi, *Science*, 2010, **329**, 424; H. K. Chae, D. Y. S. Pérez. J. Kim, Y. Go, M. Eddaoudi, A. J. Matzger, M. O'Keeffe, and O. M. Yaghi, *Nature*, 2004, **427**, 523.

15 A. M. Davis, and S. J. Teague, *Angew. Chem. Int. Edit.*, 1999, **38**, 737.

16 S. Shimomura, S. Horike, R Matsuda, and S. Kitagawa, *J. Am. Chem. Soc.*, 2007, **129**, 10990.

17 S. Furukawa, K. Tahara, F. C. De Schryver, M. Van der Auweraer, Y. Tobe, and S. De Feyter, *Angew. Chem. Int. Edit.*, 2007, **46**, 2831.

18 D. den Boer, M. Li, T. Habets, P. Iavicoli, A. E. Rowan, R. J. M. Nolte, S. Speller, D. B. Amabilino, S. De Feyter, and J. A. A. W. Elemans, *Nature Chemistry*, 2013, **5**, 621; A. Miura, S. De Feyter, M. M. S. A. Mottaleb, A. Gesquière, P. C. M. Grim, G. Moessner, M. Sieffert, M. Klapper, K. Müllen, and F. C. De Schryver, *Langmuir*, 2003, **19**, 6474.

19 L. Chen, H. Li, and A. T. S. Wee, *ACS Nano* 2009, **3**, 3684; J. M. MacLeod, J. L. Duffin, C. Y. Fu, and F. Rosei, *Acs Nano* 2009, **3**, 3347.

20 M. Li, Y. L. Yang, K. Q. Zhao, Q. D. Zeng, and C. Wang, *J. Phys. Chem. C*, 2008, **112**, 10141.

21 S. L. Johnson, and K. A. Rumon, *J. Phys. Chem.*, 1965, **69**, 74.

22 T. Kato, and J. M. J. Frechet, *J. Am. Chem. Soc.*, 1989, **111**, 8533.

23 P. C. Painter, J. Y. Lee, and M. M. Coleman, *Macromolecules*, 1988, **21**, 954.

24 A. D. Becke, *J. Chem. Phys*., 1988, **88**, 2547.

25 J. P. Perdew, and Y. Wang, *Phys. Rev. B*, 1992, **45**, 13244.

26 S. Griessl, M. Lackinger, M. Edelwirth, M. Hietschold, and W. M. Heckl, *Single Mol.*, 2002, **3**, 25.

27 L. Kampschulte, S. Griessl, W. M. Heckl, and M. Lackinger, *J Phys. Chem. B*, 2005, **109**, 14029.

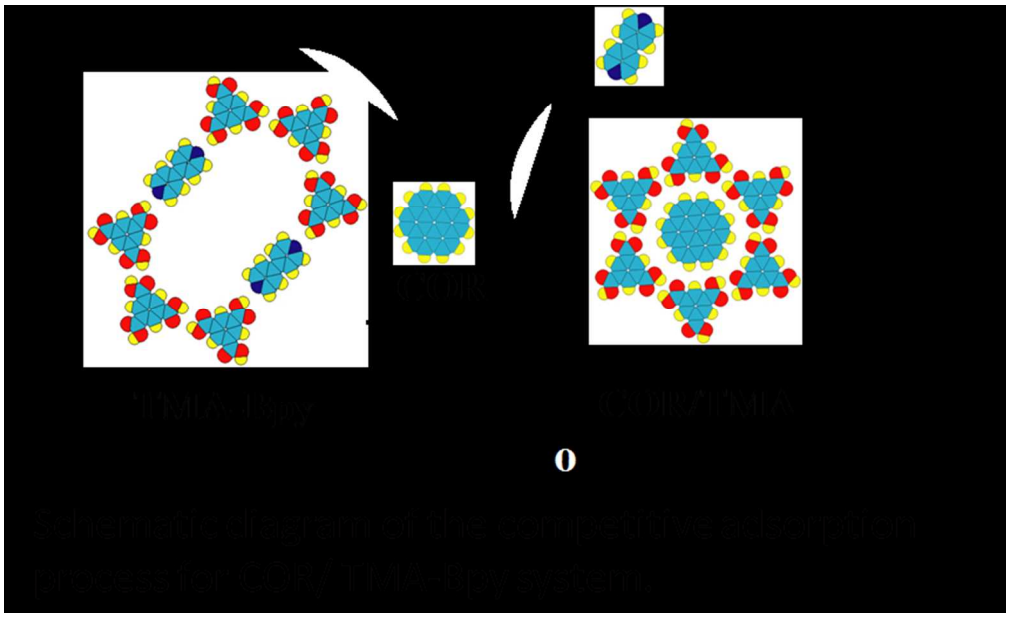

Schematic diagram of the competitive adsorption process for COF/TMA-Bpy system.

144x87mm (150 x 150 DPI)